Int. J. Heat Mass Transfer. Vol. 21, pp. 1421–1430

0017-9310/78/1101-1421 $02.00/0

ANALYSIS OF SOLIDIFICATION INTERFACE SHAPE DURING CONTINUOUS CASTING OF A SLAB

ROBERT SIEGEL
National Aeronautics and Space Administration, Lewis Research Center, Cleveland, Ohio 44135, U.S.A.

(*Received* 15 *December* 1977 *and in revised form* 26 *April* 1978)

Abstract—An analysis was made of the two-dimensional interface shape of a slab ingot being cast continuously by withdrawing it from a mold. The sides of the ingot are being cooled and the upper boundary of the ingot is in contact with a pool of molten metal. The solidification interface shape was determined from the analysis of the heat flow, utilizing the condition that the solidification interface is at constant temperature and must be normal to the lines of heat flow carrying away latent heat of fusion from the interface. The analysis includes the effect of interface curvature which, for a constant rate of withdrawing the cast ingot from the mold, causes the solidification to be nonuniform along the interface. The analysis was carried out by a conformal mapping procedure.

NOMENCLATURE

A, dimensionless parameter and dimensionless length, $a\bar{u}\rho\lambda/k(t_f-t_c) = a/\gamma$;
a, half-width of slab ingot;
b, vertical distance from center of solidification interface to bottom edge of mold;
C_1, C_2, C_3, C_4, constants;
c,d, values in mapping along real axis of u-plane, $c' = (1-c^2)^{1/2}$;
c_p, specific heat of solidified material;
E, elliptic integral of the second kind;
F, elliptic integral of the first kind;
h, height from bottom edge of mold to location where interface contacts mold surface;
K, complete elliptic integral of the first kind;
k, thermal conductivity of solidified material;
n, normal to interface, $N = n/\gamma$;
t, temperature; $T = (t-t_c)/(t_f-t_c)$;
u, coordinate in u-plane;
$\bar{u}$, casting velocity of ingot;
V, intermediate mapping plane;
W, potential plane, $W = -T+i\psi$;
x,y, coordinates in physical plane, $X = x/\gamma$, $Y = y/\gamma$;
z, complex variable in physical plane, $z = x+iy$; $Z = z/\gamma$.

Greek symbols

α,β, inflection points on solidification interface;
γ, length scale parameter, $k(t_f-t_c)/\bar{u}\rho\lambda$;
δ, maximum height variation of interface, $\Delta = \delta/\gamma$;
ζ, complex derivative, $-\partial T/\partial X + i\,\partial T/\partial Y$;
Θ, theta function defined in equation (B7) in Appendix B;
θ, angle between interface normal and ingot centerplane, Fig. 2;
λ, latent heat of fusion per unit mass of solid;
ξ,η, coordinates of u-plane;
ρ, density of solidified material;
τ, time;
ϕ, amplitude of elliptic integral;
ψ, ordinate in W-plane;
ω, reciprocal transformation, $1/\zeta$.

Subscripts

c, at cooled boundary;
f, at solidification temperature;
s, at solidification interface.

INTRODUCTION

CONTINUOUS casting is an important metal fabrication technique as it offers a rapid production method during which some control can be made on the internal metallic structure. The crystal structure is influenced by the casting velocity and the shape of the solidification interface. These quantities are related to the effectiveness of the cooling that is provided and the geometric orientation of the cooled boundaries of the casting relative to the solidification interface. The complicated heat-transfer process has been analyzed by various mathematical and numerical techniques as given for example by [1–4].

The analysis is difficult because the shape of the solidification interface is unknown; hence the technique for solving the heat-conduction equation in the solidified ingot must enable the region shape to be determined simultaneously as part of the analysis. Some simplifications are usually made in order to approximately calculate the location of the curved interface. In [5] a conformal mapping technique was devised by which the shape of an unknown solidification interface could be analytically determined for a class of two-dimensional solidification problems. For the cooling conditions applied here at the boundaries of the ingot, it was possible to use this method to obtain an exact solution for the interface shape. The shape was found to depend only on a single parameter containing the casting rate, width of

the ingot and temperature drop from the interface to the cooled boundary. The form of the parameter shows the interaction of these variables in affecting the interface shape.

The present paper is a continuation of the work recently published in [6]. The previous paper dealt with a particular type of casting process where there was substantial heat addition to the solidification interface from the molten metal that was being maintained superheated. This caused the heat conducted away from the interface to be always close to uniform along the interface. In the present paper an ordinary ingot casting process is considered, and the casting rates are high enough to produce significant interface curvature. This causes a variation along the interface in the local amount of heat of fusion that is being removed as the casting is formed.

For high casting rates there is experimental evidence [1] that the thickness of the solidified region increases along the mold in proportion to the square root of the distance from the location where solidification starts. The present results for high rates show that this is a good approximation for the shape of most of the solidified region.

ANALYSIS

An ingot in the form of a slab is being formed by continuous casting as shown in Fig. 1. The mold walls are assumed to be of insulating material, and there is often poor contact of the walls with the ingot due to metal contraction. As a result most of the heat flow associated with the change of phase from liquid to solid at the solidification interface is transferred down and outward through the cooled sides of the ingot. It is assumed that these sides are cooled by a good heat-transfer medium such as a liquid spray or a liquid metal so that the sides are essentially at a uniform temperature t_c.

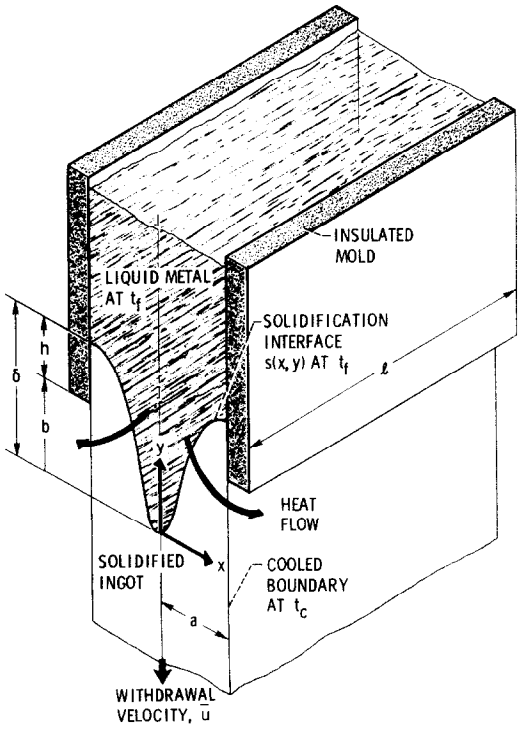

FIG. 1. Slab ingot being withdrawn from a mold in continuous casting.

The ingot is being cast continuously at a uniform rate; hence the vertical thickness of material formed at the interface at each x in a time $d\tau$ is $\bar{u}\,d\tau$, where $\bar{u}$ is the ingot casting velocity. The latent heat of fusion that must be removed per unit time and per unit area on the interface is then $\rho\lambda\bar{u}\cos\theta$ where θ is the angle between the normal to the interface and the y-axis (see Fig. 2). The temperature of the molten metal above the interface is specified to be at or only a little above the melting point, so that the only heat

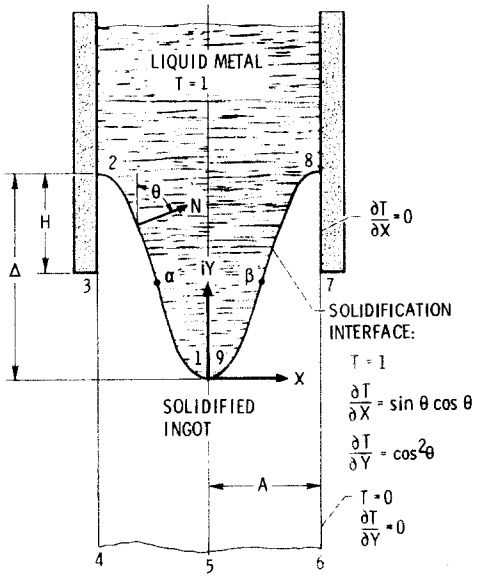

FIG. 2. Ingot geometry and boundary conditions in dimensionless physical plane, $Z = X + iY$.

flowing across the interface and into the solid is due to the solidification process. Since the interface is isothermal this heat flow is locally normal to the interface. Hence the boundary condition at each location along the interface is

$$k\left.\frac{\partial t}{\partial n}\right|_s = \rho\lambda\bar{u}\cos\theta. \tag{1}$$

Using the relations from ([7] p. 7) that $\partial t/\partial x = (\partial t/\partial n)\sin\theta$ and $\partial t/\partial y = (\partial t/\partial n)\cos\theta$, equation (1) can be resolved into two components

$$\left.\frac{\partial t}{\partial x}\right|_s = \left.\frac{\partial t}{\partial n}\right|_s \sin\theta = \frac{\rho\lambda}{k}\bar{u}\sin\theta\cos\theta \tag{2a}$$

$$\left.\frac{\partial t}{\partial y}\right|_s = \left.\frac{\partial t}{\partial n}\right|_s \cos\theta = \frac{\rho\lambda}{k}\bar{u}\cos^2\theta. \tag{2b}$$

A second condition along the interface is that the temperature is constant and equal to the melting temperature,

$$t(x_s, y_s) = t_f. \tag{3}$$

Along the cooled boundaries of the ingot the temperature is constant

$$t(x, y) = t_c \quad (x = \pm a, y < b). \tag{4}$$

Along the portion of the ingot sides that are within the mold, it is assumed that there is negligible outward heat flow so that

$$\left.\frac{\partial t}{\partial x}\right|_y = 0 \quad (x = \pm a, y > b). \tag{5}$$

This condition follows from the fact that the mold is often made of a material that is not a good heat conductor. Also after solidification, the solid metal begins to contract and pull away from the mold surface producing an insulating air gap.

At the interface, for the material that is solidified in a unit width of the x direction, the rate at which latent heat must be removed through the solid is $\rho\bar{u}\lambda$. The maximum rate at which energy can be carried as heat capacity by the motion of the ingot is the transport at the maximum temperature above the coolant temperature, $\rho\bar{u}c_p(t_f - t_c)$. The relative magnitude of the heat flow from latent heat removal as compared to the heat capacity transport is thus $\rho\bar{u}\lambda/\rho\bar{u}c_p(t_f - t_c) = \lambda/c_p(t_f - t_c)$. This is independent of the ingot withdrawal velocity. There are many instances where $\lambda/c_p(t_f - t_c)$ is sufficiently large that the dominating mode of heat flow is by conduction. Then the temperature distribution within the solid is governed by the heat conduction equation

$$\frac{\partial^2 t}{\partial x^2} + \frac{\partial^2 t}{\partial y^2} = 0. \tag{6}$$

Additional discussion will be given later on the required magnitude of $\lambda/c_p(t_f - t_c)$ for equation (6) to govern the heat flow process.

Ordinarily in the solution of Laplace's equation, either the temperature or the temperature derivative is independently specified on each boundary. In the present situation there is both a specified temperature t_f and a specified normal derivative, $\rho\lambda\bar{u}\cos\theta/k$ from equation (1), and it is the unknown shape of the freezing interface that must be determined. This will be obtained by a conformal mapping procedure that is adapted from that devised in [5].

Conformal mapping method

It is convenient in the conformal mapping method to use dimensionless variables which are chosen to simplify the boundary conditions. A dimensionless temperature is defined as $T = (t - t_c)/(t_f - t_c)$ so that $T = 1$ along the solidification interface, and $T = 0$ along the cooled boundary. A length scale parameter is defined as $\gamma = k(t_f - t_c)/\bar{u}\rho\lambda$ and the dimensionless lengths then become $X = x/\gamma$, $Y = y/\gamma$, and $N = n/\gamma$. Equations (2) become

$$\frac{\partial T}{\partial X} = \sin\theta\cos\theta \tag{7a}$$

$$\frac{\partial T}{\partial Y} = \cos^2\theta. \tag{7b}$$

These conditions along with the other boundary conditions are shown in Fig. 2. A relation that will be needed later is to note from equations (7) that

$$\left(\frac{\partial T}{\partial X}\right)^2 + \left(\frac{\partial T}{\partial Y}\right)^2 = \cos^2\theta = \frac{\partial T}{\partial Y}$$

which gives along the solidification interface,

$$\left(\frac{\partial T}{\partial X}\right)^2 + \left(\frac{\partial T}{\partial Y} - \frac{1}{2}\right)^2 = \left(\frac{1}{2}\right)^2. \tag{8}$$

The general ideas for applying conformal mapping to some types of solidification problems were

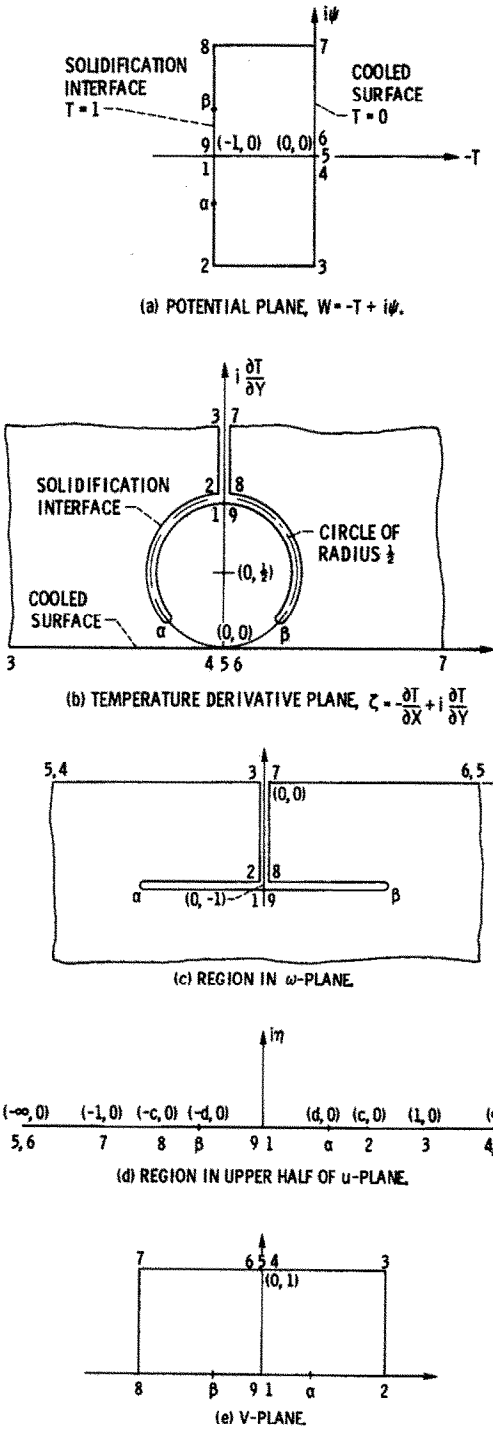

FIG. 3. Planes used in conformal mapping procedure.

developed in [5]. The direction of positive heat flow is in the direction of the gradient of the negative temperature. Hence from the definition of a potential function which relates local flow to the local gradient of a quantity producing the flow, the quantity $-T$ is the potential function for heat flow. From complex variable theory the potential function can be used as the real part of an analytic function of a complex variable

$$W = -T + i\psi \tag{9}$$

and this function satisfies Laplace's equation.

If the solidified ingot is mapped into the W-plane it forms a rectangle as shown in Fig. 3(a) where the numbered points correspond to those in Fig. 2. The solidification interface and the cooled surfaces form vertical constant temperature lines. The insulated boundaries $\overline{23}$ and $\overline{78}$ in Fig. 3(a) are normal to the constant temperature lines. Since no heat flow crosses the insulated boundaries, these boundaries are along the direction of heat flow, this direction being normal to the lines of constant temperature. The isotherms in Fig. 3(a) are a known set of vertical lines. In the analysis, this rectangle will be conformally mapped into the physical plane and the isotherms in the physical geometry obtained from the mapping of the vertical constant temperature lines. The particular isotherm of main interest is along the solidification interface, and thus the shape of the interface will be found in the physical plane.

To relate the potential and physical planes [Figs. 3(a) and 2], begin with the derivative of equation (9), $dW/dZ = -\partial T/\partial X + i\,\partial\psi/\partial X$. By use of the Cauchy–Riemann equation $\partial\psi/\partial X = \partial T/\partial Y$, this becomes

$$\frac{dW}{dZ} = -\frac{\partial T}{\partial X} + i\frac{\partial T}{\partial Y} \equiv \zeta. \tag{10}$$

Integrating yields

$$Z = \int \frac{1}{\zeta} dW + C_1. \tag{11}$$

This integration provides the desired relation between the physical Z-plane and the potential W-plane, but the function ζ must be related to W before the integration can be carried out. The ζ involves the temperature derivatives and will introduce the derivative conditions at the interface given by equations (7), thus accounting for the variation in latent heat along the interface associated with the solidification.

To relate ζ to W the solidified region is drawn in the ζ-plane (Fig. 3b). Along the cooled constant temperature boundaries $\overline{34}$ and $\overline{67}$, $\partial T/\partial Y = 0$; hence these boundaries are along the horizontal axis in Fig. 3(b). Similarly the lines $\overline{23}$ and $\overline{78}$ are along the vertical axis. Equation (8) describes a circle with a radius of 1/2 and with its center at $\partial T/\partial Y = 1/2$, $\partial T/\partial X = 0$. The interface doubles back along this circle at the inflection points α and β along the surface. The relation between ζ and W can be obtained by conformally mapping the region in Fig. 3(b) into the rectangle of Fig. 3(a).

As a first step in the mapping, a reciprocal transformation is used

$$\omega = \frac{1}{\zeta}. \tag{12}$$

Then along the circular interface in the ζ-plane

$$\omega = \frac{1}{\zeta} = \frac{1}{-\dfrac{\partial T}{\partial X} + i\dfrac{\partial T}{\partial Y}} = \frac{-\dfrac{\partial T}{\partial X} - i\dfrac{\partial T}{\partial Y}}{\left(\dfrac{\partial T}{\partial X}\right)^2 + \left(\dfrac{\partial T}{\partial Y}\right)^2}.$$

Using equations (7) and (8)

$$\omega = \frac{-\sin\theta\cos\theta - i\cos^2\theta}{\cos^2\theta} = -\frac{\sin\theta}{\cos\theta} - i.$$

Thus along the interface, the imaginary part of ω is a constant, $-i$, and the circle in Fig. 3(b) is along a horizontal line at -1 in Fig. 3(c). The line $\overline{37}$ remains along the real axis with the point 5 at $\zeta = 0$ transforming to $\omega = \infty$.

The region in Fig. 3(c) is a generalized rectangle and its boundary can be unfolded to lie along the real axis in the u-plane of Fig. 3(d). The solidified region is now in the upper half-plane. This mapping is done by means of the Schwarz–Christoffel transformation ([8] pp. 365–367)

$$\frac{d\omega}{du} = C_2 \frac{(u+d)(u-d)}{(u+1)^{1/2}(u-1)^{1/2}(u+c)^{1/2}(u-c)^{1/2}}. \tag{13}$$

At $u = 0$ (points 1 and 9), $\omega = -i$, so that the integration of equation (13) yields

$$\omega(u) + i = C_2 \int_0^u \frac{u^2 - d^2}{(u^2-1)^{1/2}(u^2-c^2)^{1/2}}\,du. \tag{14}$$

By matching points 2 and 3 in the ω and u planes, the C_2 and d are obtained. The matching is done in Appendix A and gives the result

$$\omega = \frac{1}{\zeta(u)} = \frac{2K(c)}{\pi}\int_0^u \frac{\left[1 - \dfrac{E(c)}{K(c)}\right] - u^2}{(u^2-1)^{1/2}(u^2-c^2)^{1/2}}\,du - i \tag{15}$$

where E and K are elliptic integrals.

The next step in the mapping, that is being done to relate ζ to W (through the use of an intermediate variable u), is to take the real axis of the u-plane in Fig. 3(d) and fold it into the rectangle of the V-plane in Fig. 3(e). From the Schwarz–Christoffel transformation, the relation between V and u can be found from

$$\frac{dV}{du} = \frac{C_4}{(u-c)^{1/2}(u+c)^{1/2}(u-1)^{1/2}(u+1)^{1/2}}. \tag{16}$$

The final transformation in the mapping relates Figs 3(a) to (e). By rotation and translation, this transformation is

$$W = -iV - 1. \tag{17}$$

All the required mappings are now available to transform the known rectangle of Fig. 3(a) into the physical plane of Fig. 2 and thereby obtain the unknown shape of the solidification interface. To be able to carry out the integration, equation (11) is written as

$$Z = \int \frac{1}{\zeta(u)} \frac{dW}{dV} \frac{dV}{du} du + C_1. \tag{18}$$

At $Z = 0$, $u = 0$ so this can be written as

$$Z = \int_0^u \frac{1}{\zeta(u)} \frac{dW}{dV} \frac{dV}{du} du. \tag{19}$$

Inserting equations (15)–(17) gives

$$Z = \int_0^u \left\{ \frac{2K(c)}{\pi} \int_0^u \frac{\{1-[E(c)/K(c)]\}-\xi^2}{(\xi^2-1)^{1/2}(\xi^2-c^2)^{1/2}} d\xi - i \right\} \frac{(-i)C_4}{(u^2-c^2)^{1/2}(u^2-1)^{1/2}} du. \tag{20}$$

The coordinates of the solidification interface can be found by integrating equation (20) along the real axis for values of u such that $0 < |u| < c < 1$. The integration is done in Appendix B and results in the following relations for the coordinates along the interface,

$$\left.\begin{aligned} X_s/A &= \pm F(\phi, c)/K(c) \\ Y_s/A &= (2/\pi)\ln\{\Theta[F(\phi, c)]/\Theta(0)\} \end{aligned}\right\} \quad \begin{aligned} \phi &= \sin^{-1}(u/c) \\ 0 &\leqslant u \leqslant c \end{aligned} \tag{21a, 21b}$$

where F is an elliptic integral and Θ is the theta function.

The quantity c is a location along the real axis in Fig. 3(d) and to be meaningful, the c must be related to physical quantities. This can be done by noting that the width of the rectangle in Fig. 3(a) must be unity as fixed by the dimensionless temperature difference. Thus from Fig. 3(a), $W(3)-W(2) = 1$. By noting that points 2 and 3 are at $u = c$ and $u = 1$ in Fig. 3(d), this equality can be written as

$$1 = \int_c^1 \frac{dW}{dV} \frac{dV}{du} du. \tag{22}$$

Substituting relations from equations (16) and (17) into equation (22) gives

$$1 = \int_c^1 [-iC_4/(u^2-1)^{1/2}(u^2-c^2)^{1/2}] du. \tag{23}$$

The C_4 was found in Appendix B as $C_4 = -A/K(c)$, and in the range between c and 1 ($c \leqslant u \leqslant 1$), equation (23) can be written as

$$1 = \frac{A}{K(c)} \int_c^1 \frac{du}{(1-u^2)^{1/2}(u^2-c^2)^{1/2}} = A \frac{K(c')}{K(c)}. \tag{24}$$

The final form of equation (24) was obtained by noting that the integral is a form of the complete elliptic integral of the first kind. Substituting for A (which is a dimensionless length) in terms of its physical equivalent, gives the relation between the physical variables and the parameter c used in the mapping,

$$A = \frac{a\bar{u}\rho\lambda}{k(t_f - t_c)} = \frac{K(c)}{K(c')}. \tag{25}$$

In addition to the coordinates of the interface given by equations (21), there is one remaining quantity to be found before the interface geometry is completely determined; this is the height H of the interface above the bottom edge of the mold as shown in Fig. 2. This height is equal to $\mathcal{I}m[Z(2)-Z(3)]$, where points 2 and 3 correspond to $u = c$ and $u = 1$ along the real axis of Fig. 3(d). Then from equation (20) with $C_4 = -A/K(c)$ inserted from Appendix B,

$$\begin{aligned} \mathcal{I}m\left[\frac{Z(2)-Z(3)}{A}\right] = \frac{H}{A} &= \mathcal{I}m\left(\frac{1}{K(c)} \int_1^c \left\{ \frac{2K(c)}{\pi} \frac{\{1-[E(c)/K(c)]\}-\xi^2}{(\xi^2-1)^{1/2}(\xi^2-c^2)^{1/2}} d\xi - i \right\} \frac{i}{(u^2-c^2)^{1/2}(u^2-1)^{1/2}} du\right) \\ \frac{H}{A} = \frac{h}{a} &= \mathcal{I}m\left[\frac{1}{K(c)} \int_c^1 \left\{ \frac{2K(c)}{\pi} \int_0^u \frac{\xi^2-\{1-[E(c)/K(c)]\}}{(\xi^2-1)^{1/2}(\xi^2-c^2)^{1/2}} d\xi + i \right\} \frac{du}{(1-u^2)^{1/2}(u^2-c^2)^{1/2}}\right]. \end{aligned} \tag{26}$$

The integration in equation (26) is carried out in Appendix C and yields the result

$$\frac{h}{a} = \frac{H}{A} = \frac{1}{2A} + \frac{1}{\pi}\ln\left(\frac{1}{c}\right). \tag{27}$$

RESULTS AND DISCUSSION

To obtain the geometry of the solidification interface, equation (25) is used first. Various c values are inserted on the right side and this gives the corresponding values of the physical parameter, $A = a\bar{u}\rho\lambda/k(t_f - t_c)$. The A is the single governing parameter upon which the interface shapes depend. Then for a given A the corresponding c is found and inserted into equations (21) to find the interface shape. To locate the position of the interface in the mold, the height of the interface above the bottom edge of the mold is found from equation (27). These

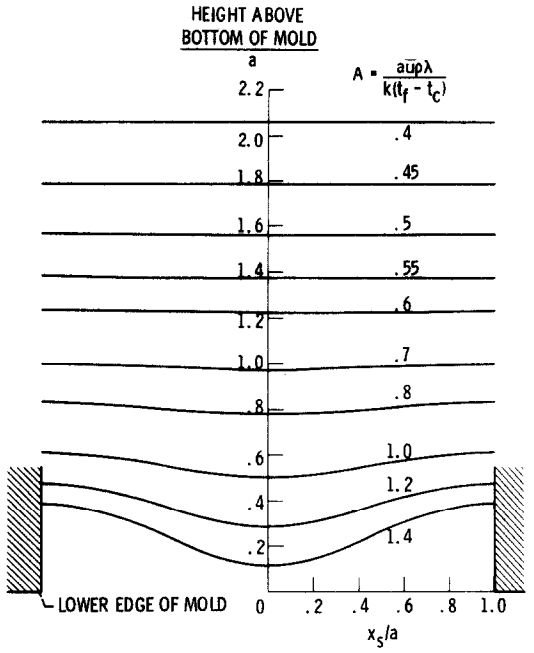

(a) $0.4 \leq A \leq 1.4$.

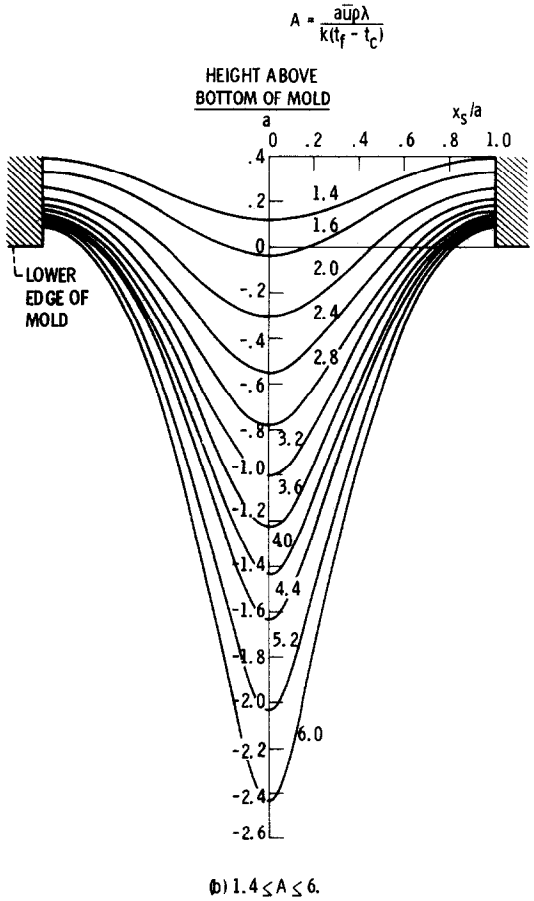

(b) $1.4 \leq A \leq 6$.

FIG. 4. Shape of solidification interface for various values of A.

calculations were carried out for various A values and the interfaces are shown in Fig. 4.

The neglect of energy transport in the form of heat capacity was discussed relative to equation (6) and is now considered in more detail. The energy equation including the transport term $u\partial t/\partial x$ is, in the dimensionless system

$$\frac{c_p(t_f - t_c)}{\lambda}\frac{\partial T}{\partial X} = \frac{\partial^2 T}{\partial X^2} + \frac{\partial^2 T}{\partial Y^2}.$$

This reduces to Laplace's equation for small $c_p(t_f - t_c)/\lambda$ (small Stefan number) as was discussed physically prior to equation (6). Although it is for a somewhat different situation of freezing of a slab, the results in [9] indicate that for heat conduction to be dominating over heat transport, the $c_p(t_f - t_c)/\lambda$ should be less than 2/3. Then as an example, for nickel, $\lambda \approx 310\,\text{kJ/kg}$ and $c_p \approx 0.46\,\text{kJ/kg}\,^\circ\text{C}$, the $t_f - t_c$ has to be less than $2\lambda/3c_p = 449^\circ\text{C}$.

For a fixed width between the mold walls, a fixed temperature difference, and a specified solidifying material, the parameter A is directly proportional to the casting velocity $\bar{u}$. For a small casting velocity (small A) the heat flow rate to the coolant is low. The solidification interface is up high within the mold because a low heat flow rate corresponds to a long path (high heat flow resistance) between the solidification interface and the cooled boundary. The interface is flat as the heat flow direction is nearly parallel to the mold walls. For a small A the c becomes small and c' approaches 1. Then $K(c) \to \pi/2$ and $K(c') \to \ln(4/c)$. Inserting these into equation (25) and solving for c gives $c = 4\exp(-\pi/2A)$. Then from equation (27) $h/a = (1/A) + (1/\pi)\ln(1/4)$. This gives a very good approximation for the interface height when A is less than about 0.6. For a very small A the interface height increases inversely as A is reduced, corresponding to a reduction in casting velocity.

As the casting velocity is increased, the solidification interface has to move down within the mold so that short heat flow paths to the cooled boundaries are provided to accommodate the increased heat flow. As shown in Fig. 4(b), the interface becomes shaped somewhat like a cosine curve. The central part of the interface can extend far below the lower edge of the mold and heat is then flowing almost horizontally from the interface to the cooled boundaries. These are the trends in interface behavior that have been observed in the numerical solutions in [1, 2].

If, for metallurgical considerations in regulating the internal structure of the casting it is desired to have the interface kept within a certain limit of curvature, the parameter A will provide the required limits on the casting variables. For a given solidifying material, so that ρ, λ, k, and t_f are fixed, the interface can be made more flat by decreasing a, $\bar{u}$, or t_c, each of which will decrease the value of A.

The curves of the solidification interface can be normalized by dividing the x_s and y_s coordinates by their maximum values. The resulting curves are shown in Fig. 5 for the range of A values over which the interface is appreciably curved. This set of curves shows that the interface has close to the same shape

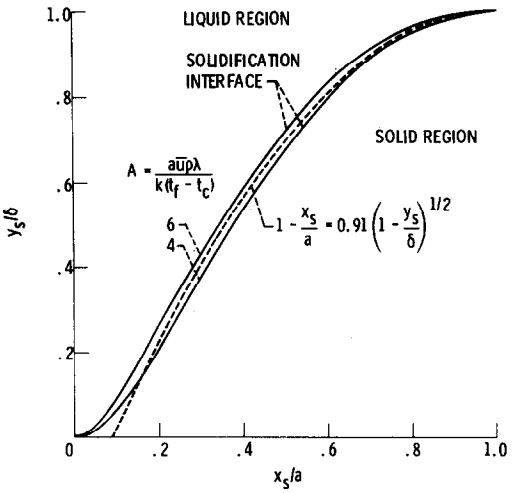

FIG. 5. Comparison of solidification interface shape with square root relation.

for all of these A values. In [1] there is some experimental data indicating that the thickness of the solidified region increases as the square root of the distance measured from the location where solidification first begins. In Fig. 5 this would mean that

$$1 - \frac{x_s}{a} = C_3\left(1 - \frac{y_s}{\delta}\right)^{1/2}$$

where C_3 is a constant. A curve is shown for $C_3 = 0.91$ and the comparison shows that the present results are quite well approximated by this square root behavior.

CONCLUSIONS

An analysis was carried out to determine the shape of the solidification interface in a continuous casting process. The shape was found to depend on only one dimensionless parameter that involves the casting rate, the width of the ingot, and the cooled boundary temperature imposed by the coolant. This parameter governs the curvature of the solidification interface and thus shows what conditions must be imposed to achieve a desired flatness of the interface; the flatness has an influence on the microscopic crystal growth at the interface. The thickness of the solidified material was found to increase approximately as the square root of the distance along the mold from the location where solidification begins; this behavior has been observed experimentally as documented in the literature.

REFERENCES

1. E. A. Mizikar, Mathematical heat transfer model for solidification of continuously cast steel slabs, *Trans. Metall. Soc. A.I.M.E.* **239**, 1747–1753 (1967).
2. D. J.-P. Adenis, K. H. Coats and D. V. Ragone, An analysis of the direct-chill-casting process by numerical methods, *Inst. Met.* **91**, 395–403 (1962–3).
3. A. A. Sfeir and J. A. Clumpner, Continuous casting of cylindrical ingots, *J. Heat Transfer* **99**, 29–34 (1977).
4. P. G. Kroeger and S. Ostrach, The solution of a two-dimensional freezing problem including convection effects in the liquid region, *Int. J. Heat Mass Transfer* **17**, 1191–1207 (1974).
5. R. Siegel, Conformal mapping for steady two-dimensional solidification on a cold surface in flowing liquid, NASA TN D-4771 (August 1968).
6. R. Siegel, Shape of two-dimensional solidification interface during directional solidification by continuous casting, *J. Heat Transfer* **100**, 3–10 (1978).
7. E. R. G. Eckert and R. M. Drake, Jr., *Analysis of Heat and Mass Transfer*. McGraw-Hill, New York (1972).
8. G. Moretti, *Functions of a Complex Variable*. Prentice-Hall, Englewood Cliffs, N.J. (1964).
9. F. Kreith, *Principles of Heat Transfer*, 2nd Edn, p. 477. International Textbook Co., Scranton, Pennsylvania.
10. H. B. Dwight, *Tables of Integrals and Other Mathematical Data*, 4th Edn. Macmillan, New York (1961).
11. P. F. Byrd and M. D. Friedman, *Handbook of Elliptic Integrals for Engineers and Scientists*, 2nd Edn, revised. Springer, Berlin (1971).

APPENDIX A

Determination of quantities C_2 *and* d

At point 2, $u \to c$ and $\omega = -i$. Then from equation (14)

$$0 = \frac{C_2}{-1}\int_0^c \frac{u^2 - d^2}{(1-u^2)^{1/2}(c^2-u^2)^{1/2}}\,du \quad (0 \leqslant u \leqslant c < 1) \tag{A1}$$

Integrating equation (A1) gives (by use of equations 781.01 and 781.11 in [10])

$$0 = \int_0^c \frac{u^2}{(1-u^2)^{1/2}(c^2-u^2)^{1/2}}\,du - d^2\int_0^c \frac{1}{(1-u^2)^{1/2}(c^2-u^2)^{1/2}}\,du \quad (0 \leqslant u \leqslant c < 1)$$

$$0 = K(c) - E(c) - d^2K(c).$$

Thus d is related to c by

$$d^2 = 1 - \frac{E(c)}{K(c)}. \tag{A2}$$

At point 3, $u \to 1$ and $\omega \to 0$. Then from equation (13), by integrating between points 2 and 3

$$\omega(u=1) - \omega(u=c) = i = C_2\int_c^1 \frac{u^2 - d^2}{(u^2-1)^{1/2}(u^2-c^2)^{1/2}}\,du \quad (0 < c \leqslant u \leqslant 1)$$

$$i = \frac{C_2}{i}\int_c^1 \frac{u^2 - d^2}{(1-u^2)^{1/2}(u^2-c^2)^{1/2}}\,du. \tag{A3}$$

Using equations 781.02 and 781.12 in [10], equation (A3) is integrated to yield

$$i^2 = C_2[E(c') - d^2K(c')]. \tag{A4}$$

Substituting for d^2 from equation (A2) into equation (A4) gives

$$-1 = C_2\left[E(c') - K(c') + E(c)\frac{K(c')}{K(c)}\right]. \tag{A5}$$

From [11], equation 110.10, there is the identity $E(c)K(c') + E(c')K(c) - K(c)K(c') = \pi/2$ so that equation (A5) reduces to:

$$-1 = \frac{C_2}{K(c)}\frac{\pi}{2}.$$

This gives C_2 as

$$C_2 = -\frac{2K(c)}{\pi}. \tag{A6}$$

Then by substituting equations (A2) and (A6) for d^2 and C_2, equation (14) becomes

$$\omega(u)+i=-\frac{2K(c)}{\pi}\int_0^u \frac{u^2-\{1-[E(c)/K(c)]\}}{(u^2-1)^{1/2}(u^2-c^2)^{1/2}}\,du.$$

APPENDIX B

Integration to obtain interface coordinates

In the range where $0<|u|<c<1$, equation (20) becomes along the solidification interface,

$$Z_s=\int_0^u\left\{i\frac{2K(c)}{\pi}\int_0^u\frac{\xi^2-\{1-[E(c)/K(c)]\}}{(1-\xi^2)^{1/2}(c^2-\xi^2)^{1/2}}\,d\xi+1\right\}\times\frac{C_4}{(1-u^2)^{1/2}(c^2-u^2)^{1/2}}\,du. \quad (B1)$$

From [10], equations 781.01 and 781.11, the following integrals are obtained,

$$\int_0^u\frac{\xi^2}{(1-\xi^2)^{1/2}(c^2-\xi^2)^{1/2}}\,d\xi=F\left[\sin^{-1}\left(\frac{u}{c}\right),c\right]-E\left[\sin^{-1}\left(\frac{u}{c}\right),c\right] \quad (B2)$$

$$\int_0^u\frac{1}{(1-\xi^2)^{1/2}(c^2-\xi^2)^{1/2}}\,d\xi=F\left[\sin^{-1}\left(\frac{u}{c}\right),c\right] \quad (B3)$$

where F and E are elliptic integrals of the first and second kind. Inserting these relations for the inner integral of equation (B1) gives

$$Z_s=C_4\int_0^u\left[i\frac{2K(c)}{\pi}\left\{-E\left[\sin^{-1}\left(\frac{u}{c}\right),c\right]+\frac{E(c)}{K(c)}F\left[\sin^{-1}\left(\frac{u}{c}\right),c\right]\right\}+1\right]\times\frac{1}{(1-u^2)^{1/2}(c^2-u^2)^{1/2}}\,du. \quad (B4)$$

To integrate equation (B4), integrals have to be obtained of integrands involving elliptic integrals. Using the transformation, $\phi=\sin^{-1}(u/c)$, and then equations 630.01 and 630.02 in [11] gives,

$$\int_0^u\frac{F[\sin^{-1}(u/c),c]}{(1-u^2)^{1/2}(c^2-u^2)^{1/2}}\,du=\int_0^\phi\frac{F(\phi,c)}{(1-c^2\sin^2\phi)^{1/2}}\,d\phi=\frac{[F(\phi,c)]^2}{2} \quad (B5)$$

$$\int_0^u\frac{E[\sin^{-1}(u/c),c]}{(1-u^2)^{1/2}(c^2-u^2)^{1/2}}\,du=\int_0^\phi\frac{E(\phi,c)}{(1-c^2\sin^2\phi)^{1/2}}\,d\phi=\frac{[F(\phi,c)]^2E(c)}{2K(c)}+\ln\left\{\frac{\Theta[F(\phi,c)]}{\Theta(0)}\right\} \quad (B6)$$

where Θ is the theta function,

$$\Theta(\phi,c)=1+2\sum_{m=1}^{\infty}(-1)^m q^{m^2}\cos\left[\frac{m\pi F(\phi,c)}{K(c)}\right] \quad (B7)$$

in which

$$q=e^{-\pi K(c')/K(c)}$$

and

$$\Theta(0)=\left[\frac{2c'K(c)}{\pi}\right]^{1/2}$$

Insert equations (B5), (B6), and (B3) into equation (B4) to give

$$Z_s=C_4\left\{i\frac{2K(c)}{\pi}\left[-\frac{[F(\phi,c)]^2E(c)}{2K(c)}-\ln\left\{\frac{\Theta[F(\phi,c)]}{\Theta(0)}\right\}+\frac{E(c)}{K(c)}\frac{[F(\phi,c)]^2}{2}\right]+F(\phi,c)\right\}$$

which reduces to

$$Z_s=C_4\left[F(\phi,c)-i\frac{2K(c)}{\pi}\ln\left\{\frac{\Theta[F(\phi,c)]}{\Theta(0)}\right\}\right]. \quad (B8)$$

When $u\to c$ at point 2, then $\phi\to\pi/2$ and the real part of Z_s is

$$\mathscr{R}eZ_s=C_4F\left(\frac{\pi}{2},c\right)=C_4K(c). \quad (B9)$$

The real part of Z_s at point 2 is $-A$; hence, from equation (B9)

$$C_4=-A/K(c). \quad (B10)$$

Then by substituting equation (B10) into (B8),

$$\frac{Z_s}{A}=\frac{X_s}{A}+i\frac{Y_s}{A}=-\frac{F(\phi,c)}{K(c)}+i\frac{2}{\pi}\ln\left\{\frac{\Theta[F(\phi,c)]}{\Theta(0)}\right\}. \quad (B11)$$

The Z_s is along the interface between points 1 and 2 which is in the range where X_s is negative. Since the interface is symmetric about $X=0$, equation (B11) yields, by taking the real and imaginary parts,

$$\left.\begin{aligned}\frac{X_s}{A}&=\pm\frac{F(\phi,c)}{K(c)}\\ \frac{Y_s}{A}&=\frac{2}{\pi}\ln\left\{\frac{\Theta[F(\phi,c)]}{\Theta(0)}\right\}\end{aligned}\right\}\ \phi=\sin^{-1}\left(\frac{u}{c}\right) \quad (B12a)$$

$$0\leqslant u\leqslant c \quad (B12b)$$

APPENDIX C

Integration to obtain interface height above bottom edge of mold

From Fig. 3(c) and equation (15),

$$\omega(2)-\omega(1)=0=\frac{2K(c)}{\pi}\int_0^c\frac{\{1-[E(c)/K(c)]\}-u^2}{(u^2-1)^{1/2}(u^2-c^2)^{1/2}}\,du.$$

Equation (20) can then be written

$$\frac{h}{a}=\mathscr{I}m\frac{1}{K(c)}\int_c^1\left\{\frac{2K(c)}{i\pi}\times\int_c^u\frac{\xi^2-\{1-[E(c)/K(c)]\}}{(1-\xi^2)^{1/2}(\xi^2-c^2)^{1/2}}\,d\xi+i\right\}\times\frac{du}{(1-u^2)^{1/2}(u^2-c^2)^{1/2}}. \quad (C1)$$

From [10], equations 781.02 and 781.12, the integrals needed for the inner integral are

$$\int_c^u\frac{d\xi}{(\xi^2-c^2)^{1/2}(1-\xi^2)^{1/2}}=K(c')-F\left\{\sin^{-1}\left[\frac{(1-u^2)^{1/2}}{c'}\right],c'\right\} \quad (C2)$$

$$\int_c^u\frac{\xi^2\,d\xi}{(\xi^2-c^2)^{1/2}(1-\xi^2)^{1/2}}=E(c')-E\left\{\sin^{-1}\left[\frac{(1-u^2)^{1/2}}{c'}\right],c'\right\}. \quad (C3)$$

Then inserting equations (C2) and (C3) into (C1) gives,

$$\frac{h}{a}=\mathscr{I}m\frac{1}{K(c)}\int_c^1\left\{\frac{2K(c)}{i\pi}\left[E(c')-E\left\{\sin^{-1}\left[\frac{(1-u^2)^{1/2}}{c'}\right],c'\right\}-\left[1-\frac{E(c)}{K(c)}\right]\times\left(K(c')-F\left\{\sin^{-1}\left[\frac{(1-u^2)^{1/2}}{c'}\right],c'\right\}\right)\right]+i\right\}\times\frac{du}{(1-u^2)^{1/2}(u^2-c^2)^{1/2}}.$$

This can be rearranged into,

$$\frac{h}{a}=\mathscr{I}m\frac{1}{iK(c)}\int_c^1 \times\left[\frac{2}{\pi}[K(c)E(c')-K(c)K(c')+E(c)K(c')]-1-\frac{2K(c)}{\pi}\left(E\left\{\sin^{-1}\left[\frac{(1-u^2)^{1/2}}{c'}\right],c'\right\}-\left[1-\frac{E(c)}{K(c)}\right]F\left\{\sin^{-1}\left[\frac{(1-u^2)^{1/2}}{c'}\right],c'\right\}\right)\right]\times\frac{du}{(1-u^2)^{1/2}(u^2-c^2)^{1/2}}. \quad (C4)$$

Using the identity ([11], equation 110.10),

$$K(c)E(c')-K(c)K(c')+E(c)K(c')=\frac{\pi}{2} \quad (C5)$$

equation (C4) simplifies to

$$\frac{h}{a}=\frac{2}{\pi}\int_c^1\left(E\left\{\sin^{-1}\left[\frac{(1-u^2)^{1/2}}{c'}\right],c'\right\}-\left[1-\frac{E(c)}{K(c)}\right]F\left\{\sin^{-1}\left[\frac{(1-u^2)^{1/2}}{c'}\right],c'\right\}\right)\times\frac{du}{(1-u^2)^{1/2}(u^2-c^2)^{1/2}}. \quad (C6)$$

Two integrals are needed to evaluate this expression. By using the transformation $\phi=\sin^{-1}[(1-u^2)^{1/2}/c']$ the integral involving F can be transformed into a standard form and then integrated by use of [11], equation 630.01,

$$\int_c^1\frac{F\{\sin^{-1}[(1-u^2)^{1/2}/c'],c'\}}{(1-u^2)^{1/2}(u^2-c^2)^{1/2}}du=\int_0^{\pi/2}\frac{F(\phi,c')\,d\phi}{(1-c'^2\sin^2\phi)^{1/2}}=\frac{[F(\pi/2,c')]^2}{2}=\frac{[K(c')]^2}{2}. \quad (C7)$$

Similarly by using [11], equation 630.02,

$$\begin{aligned}\int_c^1\frac{E\{\sin^{-1}[(1-u^2)^{1/2}/c'],c'\}}{(1-u^2)^{1/2}(u^2-c^2)^{1/2}}du&=\int_0^{\pi/2}\frac{E(\phi,c')\,d\phi}{(1-c'^2\sin^2\phi)^{1/2}}\\&=\frac{[F(\pi/2,c')]^2E(c')}{2K(c')}+\ln\left\{\frac{\Theta[F(\pi/2,c')]}{\Theta(0)}\right\}\\&=\frac{[K(c')]^2E(c')}{2K(c')}+\ln\left\{\frac{\Theta[K(c')]}{\Theta(0)}\right\}\\&=\frac{K(c')E(c')}{2}+\ln\left\{\frac{[2K(c')/\pi]^{1/2}}{[2cK(c')/\pi]^{1/2}}\right\}\\&=\frac{K(c')E(c')}{2}+\ln\frac{1}{c^{1/2}}.\end{aligned} \quad (C8)$$

Substituting equations (C7) and (C8) into (C6) gives for h/a,

$$\begin{aligned}\frac{h}{a}&=\frac{2}{\pi}\left\{\frac{K(c')E(c')}{2}+\ln\frac{1}{c^{1/2}}-\left[1-\frac{E(c)}{K(c)}\right]\frac{[K(c')]^2}{2}\right\}\\&=\frac{2}{\pi}\left\{\frac{K(c')}{2}\left[E(c')-K(c')+\frac{E(c)K(c')}{K(c)}\right]+\ln\frac{1}{c^{1/2}}\right\}.\end{aligned} \quad (C9)$$

Using the identity given by equation (C5) results in

$$\begin{aligned}\frac{h}{a}&=\frac{2}{\pi}\left[\frac{K(c')}{2}\frac{\pi}{2K(c)}+\ln\frac{1}{c^{1/2}}\right]\\&=\frac{1}{2}\frac{K(c')}{K(c)}+\frac{2}{\pi}\ln\frac{1}{c^{1/2}}\\&=\frac{1}{2A}+\frac{1}{\pi}\ln\left(\frac{1}{c}\right).\end{aligned} \quad (C10)$$

ANALYSE DE LA FORMATION DE L'INTERFACE SOLIDE DURANT LA COULEE CONTINUE D'UNE PLAQUE

Résumé—On analyse la formation bi-dimensionnelle de l'interface d'un lingot plat qui sort en coulée continue d'un moule. Les côtés du lingot sont refroidis et la frontière supérieure est en contact avec un volume de métal fondu. La solidification à l'interface est déterminée à partir de l'analyse du flux thermique basée sur l'hypothèse que l'interface de solidification est à température constante et qu'il est normal aux lignes de flux le long desquelles la chaleur latente de fusion quitte l'interface. L'analyse inclut l'effet de la courbure de l'interface qui, pour une vitesse de sortie constante du métal, fait que la solidification n'est pas uniforme le long de l'interface. L'étude est menée par une procédure de transformation conforme.

ANALYTISCHE BESTIMMUNG DER FORM DER ERSTARRUNGSFRONT BEIM KONTINUIERLICHEN GIESSEN EINER PLATTE

Zusammenfassung—Es wurde eine Analyse zur Bestimmung der Form der zweidimensionalen Phasengrenzfläche eines Plattenbarrens durchgeführt. Dieser wird durch Herausziehen aus einer Form kontinuierlich gegossen. Die Wände des Barrens werden gekühlt, und sein oberer Rand steht mit einem Gefäß von geschmolzenem Metall in Verbindung. Die Erstarrungsfront wurde aus der Wärmestrom–Analyse bestimmt, indem man die Bedingung benutzte, daß die Erstarrungsfront eine konstante Temperatur hat und senkrecht zur Richtung des Wärmestroms verläuft, der die Schmelzwärme von der Grenzschicht abführt. Die Analyse berücksichtigt den Effekt der Krümmung der Phasengrenze, welcher für eine konstante Abzugsgeschwindigkeit des gegossenen Barrens von der Form eine ungleichmäßige Erstarrung längs der Grenzfläche verursacht. Die Analyse wurde mittels konformer Abbildung ausgeführt.

АНАЛИЗ ФОРМЫ ПОВЕРХНОСТИ ЗАТВЕРДЕВАНИЯ В ПРОЦЕССЕ НЕПРЕРЫВНОЙ ОТЛИВКИ СЛЯБА

Аннотация — Анализируется форма двухмерной границы раздела листового слитка, получаемого методом непрерывной вытяжки из расплава. Стороны слитка охлаждаются, в то время как верхняя граница слитка соприкасается с объёмом расплавленного металла. Форма поверхности затвердевания определяется из анализа теплового потока на основании предположения о том, что эта поверхность имеет постоянную температуру и перпендикулярна направлению потока, отводящего скрытую теплоту плавления. При анализе учитывается кривизна поверхности раздела, вызывающая неравномерное затвердевание границы раздела при постоянной скорости вытяжки слитка из расплава. Анализ проводится с помощью метода конформных отображений.